Application of electrical resistivity tomography as a physicochemical tool for tailings valorisation and remediation strategies

M. Manuel[1], M. van Schoor[2], J. Amaral Filho[3], and S. Harrison[3]

[1]Mintek, South Africa
[2]Council for Scientific and Industrial Research, South Africa
[3]University of Cape Town, Cape Town

Spatial models may be used to better understand tailings' properties and identify the commodity potential in tailings storage facilities (TSF). However, this is not easily achieved as a large database of bulk assays from extensive geochemical sampling is required. Costs and time associated with large geochemical databases may be reduced through the application of ground geophysical surveys. Electrical resistivity tomography (ERT) is a well-known ground survey used to image subsurface structures, and changes in material from electrical resistivity and electromagnetic radiation measurements, respectively. These methods are typically used for geotechnical studies and archaeological applications. The objective of this study is to apply geochemical survey tools for *tailings valorisation and remediation* applications, particularly nature-based technologies. ERT data may be calibrated from calculated regression models for various physicochemical properties (distribution of metals, clays, and salinity and moisture). As such, limited physiochemical data (salinity, clay content, particle size distribution, metal concentration, and moisture) in Witwatersrand Basin tailings ponds were augmented with ERT data. This capability informs the engineered pedogenesis strategy to maximise phytoextraction.

INTRODUCTION

Nearly 25% of South Africa's population resides in Gauteng and may be exposed to elevated levels of toxic metals from 200 gold mine dumps (Minerals Council South Africa, 2019). Chronic ingestion of toxic metalloids such as arsenic has detrimental effects on all life forms and is strongly linked to hyperpigmentation, keratosis, and increased risk of skin, internal organs, lung cancers, cardiovascular disease, and neuropathy (Kapaj, Petersen & Liber, 2006).

The occurrence of metals and metalloids in tailings storage facilities (TSFs) of the Witwatersrand Basin has been reported, but the extent of toxicity is unclear. Of three sites studied by Fashola and Bablolo (2020), the Tudor shaft site had a concentration of metals; Co, Zn, Pb, As and Ni, which exceeds the permissible levels recommended by South African standards for soils and sediment quality to protect human and environmental health. The recommended standard of Contaminated Land and Soil Quality for arsenic and lead is 5.8 ppm and 20 ppm, respectively, while a composite sample from the Tudor Shaft Tailings dam sample contained 261 ppm of arsenic and ~46 ppm of lead. The sample collected was reported to be representative of the tailings dam, but there is no evidence of the spatial distribution of the toxic metals. An attempt to address this limitation was made in Netshiongolwe (2018), whereby samples were collected from the top horizon and across the adjacent tailings' footprints. Classical statistics were applied to correlate the TSF data with the tailing footprint soils, but the spatial distribution of the metalloids, and the ion exchange capacity across tailings dump that influence the mobility of the elements were not determined.

This limitation is prevalent in most studies, largely due to geochemical sampling and analyses' cost and time constraints. As such, alternative technologies to characterise and monitor TSFs should be evaluated.

Deep learning classification coupled with remote sensing imagery from satellites, radar, and infrared may be used to monitor tailings ponds, but these are only practical for large spatial areas, as the resolution is too low (Lyu *et al*., 2021). These remote technologies are more cost-effective, but links with contaminant bioavailability cannot be made. Ground geophysical surveys are hence more applicable for a more in-depth analysis of a TSF. Radiometrics are used to measure cesium, thorium, and potassium radiation, magnetometers calculate magnetic fields and gravity radiometry determine variations in gravitational acceleration on the Earth's surface, but these geophysical techniques are rarely applied to remediation projects. Electrical resistivity tomography (ERT) has however been used in a range of environmental studies related to monitoring and remediation. It can monitor risks related to river embankments (Jodry *et al.,* 2019), investigate the migration of leachate from a landfill (Maurya *et al*., 2017) and characterise mine tailings ponds based on physicochemical properties (Gabarron *et al*., (2020).

Electrical resistivity is a relatively simple technology that measures how strongly materials resist an electric current. Several combined soil properties such as clay/mineral content, porosity, texture, moisture content, solute concentration and temperature can impact electrical resistivity in different ways and to different extents. The relationship between resistivity and tailings physiochemical properties (salinity, clay content and metal concentration, cation exchanges and moisture) was successfully established using calculated regression models (Gabarron *et al.,* (2020). The authors developed a highly complex model that integrates the spatial and physicochemical properties of the ponds of a TSF. Spatial models were used to better understand tailings' properties, identify the commodity potential of the waste, explore bioremediation strategies, and rehabilitate Acid Mine drainage-affected sites. The strategies may include soil amendments that can immobilise contaminants or nature-based extraction technologies. Phytoremediation is a nature-based technology that involves the hyperaccumulation of metal as a removal mechanism of metals from polluted soil. Phytoremediation is largely dependent on oxidation states of the toxic metals, soil pH, exchange reactions, retention, mobility, and bio-accessibility of both metals and metalloids in soil. Further work is required to establish the applicability of this technique to the Witwatersrand Basin tailings ponds.

This study aims to apply geochemical survey tools for *tailings valorisation and remediation* applications, particularly nature-based technologies. In this paper, we present the case study of a TSF in the West Rand of the Witwatersrand Gold Basin in South Africa. The Witwatersrand tailings storage facilities were constructed using a paddock construction method to reduce the dispersion of metals. Over the years, an oxidation profile with three zones developed; oxidised (primarily 3 m deep), transitional and reduced (Nengovhela *et al*., 2006). The oxidised zone is of interest for bioremediation technology applications.

EXPERIMENTAL METHODS

The study site is located southwest of Johannesburg, South Africa. The area of the TSF is 2.69 km^2 and is surrounded by residential areas within a 500 m radius (Figure 1). The northern, western and eastern slopes are well-vegetated, while sparse vegetation and subsequent landslides are evident on the southern slope of the TSF (Figure 1). The slope has eight terraces, but only two were characterised to demonstrate the potential of the ERT technique. The selected terraces were visually different in colour and texture. The green terrace appeared to be more heterogeneous in colour with variable drainage patterns. The yellow terrace appeared to be more homogenous in colour and texture.

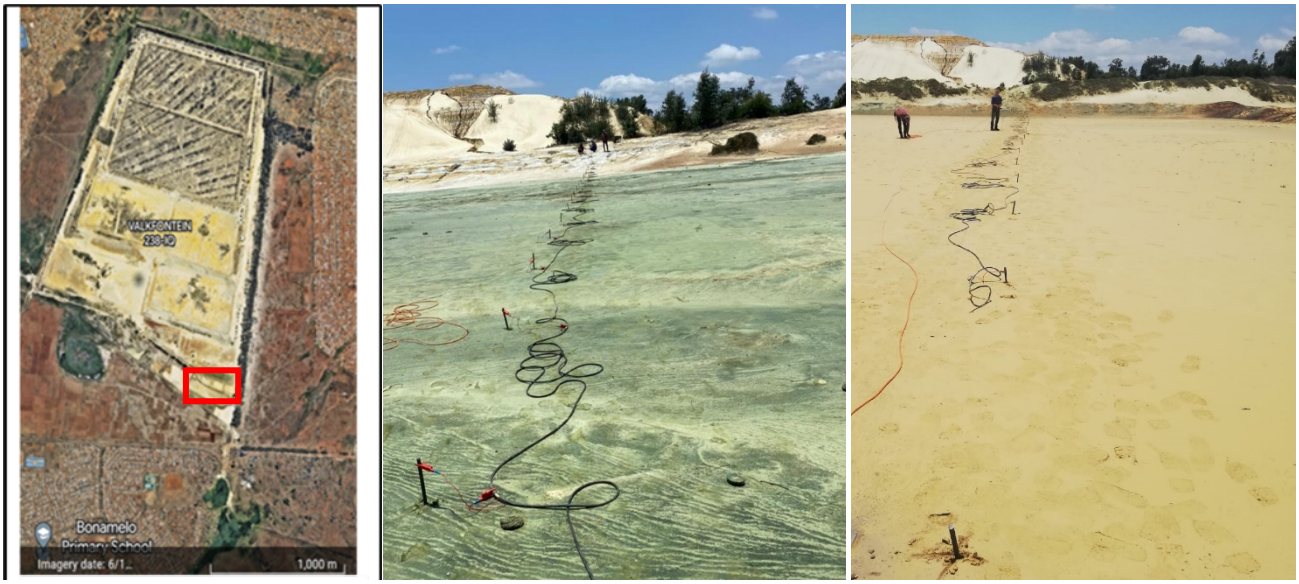

Figure 1. Electrical resistivity tomography tests on two terraces of the TSF (left) green terrace and (right) yellow terrace.

Electrical Resistivity Tomography

The electrical resistivity measurements were made by passing a current into the ground via two current electrodes and measuring the resulting voltage at two potential electrodes, a minimum of four electrodes were thus required. A total of 46 electrodes were spaced within 3 m intervals, which covered 146 m. Current electrode (AB) separations of 9 m, 18 m, 27 m and 46 m were used. The associated potential measurement electrode (MN) spacing was 3 m (for AB = 9 and 18 m) or 6 m (for AB = 27 m and 46 m). The ERT receiver used was a Zonge GDP-32^{II} multi-channel system with a Zonge ZT-30 transmitter. The ERT profile was conducted with a multi-gradient measurement scheme.

To calibrate the ERT data, samples from every fifth electrode were collected using an auger drill. The augers were manually drilled into the ground to depths of up to 60 cm. The samples along the berm slopes were collected and analysed but not reported, as they were not representative of the terraces. The samples were analysed by chemical and mineralogical methods to determine the material properties that influence resistivity, abundance of trace metals, salinity and clay. The berm samples were collected but data was not included due to heterogeneity of samples on a slope.

Water holding capacity.

The terraces were saturated due to heavy rains a week before the ERT survey and moisture analysis in the field was not determined. Determining the samples' water-holding capacity was indicative of the terrace porosity. 100 ml of dried sample was placed in a funnel and subjected to 100 ml of water. The dripping water was captured by a graduated funnel over 24 hours.

Chemical and mineralogical methods

All the samples were dissolved in aqua-regia (HCl-HNO_3-H_2O), and the leachates were measured by Inductive Coupled Plasma Mass Spectroscopy to determine 12 chemical elements (Ag, As, Cd, Co, Cr, Cu, Fe, Mn, Ni, Pb, V, and Zn) and Au prepared by fire assay and solutions measured by Inductive Coupled Plasma Optical Emission Spectroscopy. The detection limit for the base metals is 10 ppm, while the detection limit for Au is 0.08 ppm.

The mineral composition of all samples was analysed by X-ray diffraction using a Bruker D8 Advance powder diffractometer, with Lynxeye detector divergence- and fixed receiving slits with Fe-filtered Co-Kα radiation. The samples were run from 4 to 80° 2θ, with a step size of 0.02° 2θ and a counting time of 3 seconds per step. The method makes use of the net intensity of the main peaks of the phases, and

identification is based on the crystal structure of **crystalline** phases which occur in amounts of >1 mass %. Amorphous phases are not identified with this method, however, all minerals have been accounted for, by automated scanning electron microscopy.

The X-ray diffraction data was validated by automated scanning electron microscopy, QEMSCAN. Automated image analysis utilises Backscattered Electron and Energy Dispersive X-ray signals to create digital images in which each pixel corresponds to a mineral species in the corresponding region under the electron beam. QEMSCAN PMA measurement mode was used for the bulk modal analyses. This method locates all minerals using pre-defined compositional and BSE criteria in a species identification protocol list. The detection limit of this technique is approximately 0.1 mass %. The particle sizes of the samples were also determined.

It must be noted that the descriptions and quantitative data from the QEMSCAN are derived from two-dimensional measurements (x, y) from the surfaces of the polished sections. Waterless sample preparation techniques were employed to avoid the dissolution of saline minerals. Samples were mounted into polished sections for particle map analysis (PMA). The PMA technique uses particle mapping to create false colour maps from which mineral properties were quantified.

A JEOL JXA-8230 Superprobe instrument was employed to determine concentrations of major and trace elements down to ~0.01 wt. % in phases of interest. Analyses were carried out using wavelength dispersive spectrometry. Oxygen was assigned stoichiometrically. Counting times of 20 seconds on peak and 5 seconds on each of the two background positions adjacent to the peak were employed at an accelerating voltage of 20 kV, and a beam current of 30 nA with the beam defocussed to a diameter of 5 µm. The system was calibrated using pure metals, elemental oxides and sulphide standards.

RESULTS

The ERT unit electrode spacing (3 m) was used to determine the pixel dimensions of the finite-element output image in Figure 2. The processed output image is based on the 2D inversion of the field data. The legend denotes the range of electrical resistivity values, with the cool colours (i.e., blue) representing areas of low resistivity values, represented in units of ohm metres (Ω-m), while warm colours (i.e., red) represent areas of high resistivity values.

There are distinct differences in subsurface resistivity between the 'green terrace' measured by electrodes 26-46 and the lower yellow terrace measured by electrodes 1-25. The 'yellow' terrace is characterised by a relatively resistive soil, of between 150 and 1750 Ω-m. The conductive green terrace has a few localised small resistive near-surface spots, but generally, the near-surface resistivity is of the order of 10-150 Ω-m. Resistivity depth information available is approximately 20-24 m, but the meaningful range of the data decreases as one moves toward the extremities of the survey array. Although the ERT data at depth warrants further investigation, characterisation of the topsoil up to 60 cm was required for the bioremediation application. The data were interpreted by comparing electrical resistivity to salinity, particle size distributions, and metal and clay content of the near-surface material.

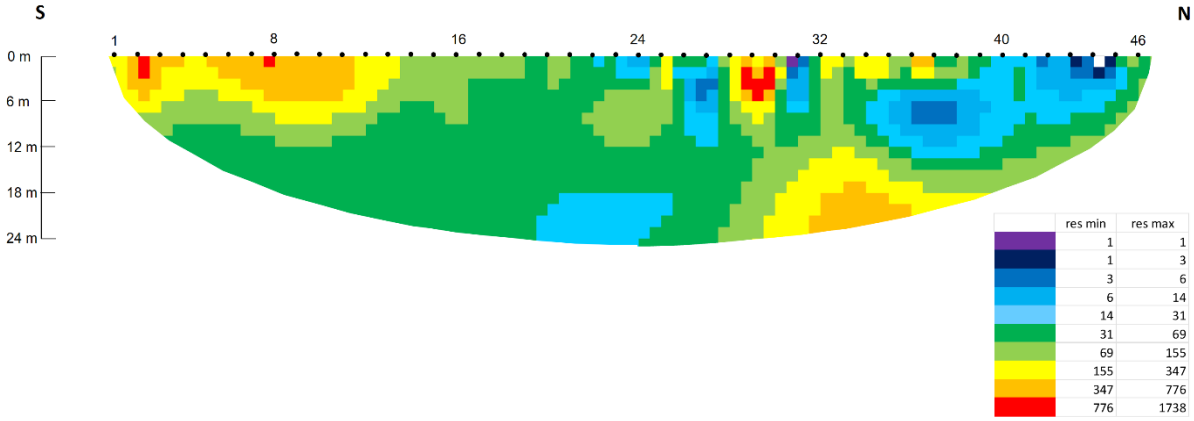

Figure 2. Processed ERT output.

Soil texture

The soil texture is defined by the particle size distribution and porosity of the tailings. The particle grain size distribution of the yellow terrace is relatively fine (Figure 3). Low resistivities are expected for fine particles, as they promote ionic current flow in saturated soil (Suddah, *et al*., 2009). Considering that the terraces were completely saturated, we can assume that the moisture of the material was equivalent to the water-holding capacity, which is between 28 and 38 %. Sandy clays with water content between 20 and 40% exhibit low resistivities, less than 100 Ω-m, while higher resistivities up to 2500 Ω-m are expected for low moisture soils (Ahn *et al*., 2022). The terraces are hence not very different in terms of moisture retention. The green terrace is slightly coarser, owed to the agglomeration of clay material. Although special care was taken to deagglomerate the particles, large (38µm) agglomerations were present. At grain size level, green terrace is relatively fine, and may be classified as clayey silt, more than 75 mass % is less than 75µm. The particle size distributions of the terraces are unlikely the reason for differences in resistivity. Resistivity values greater than 8 Ω-m correspond to coarse particles (50–2000 µm; while for fine particles (0.02–50 µm), electrical resistivity values were lower (Martinez- Pagan, *et al*., (2021). The near-uniform texture of the terraces suggests that physical parameters were not the key drivers for resistivity.

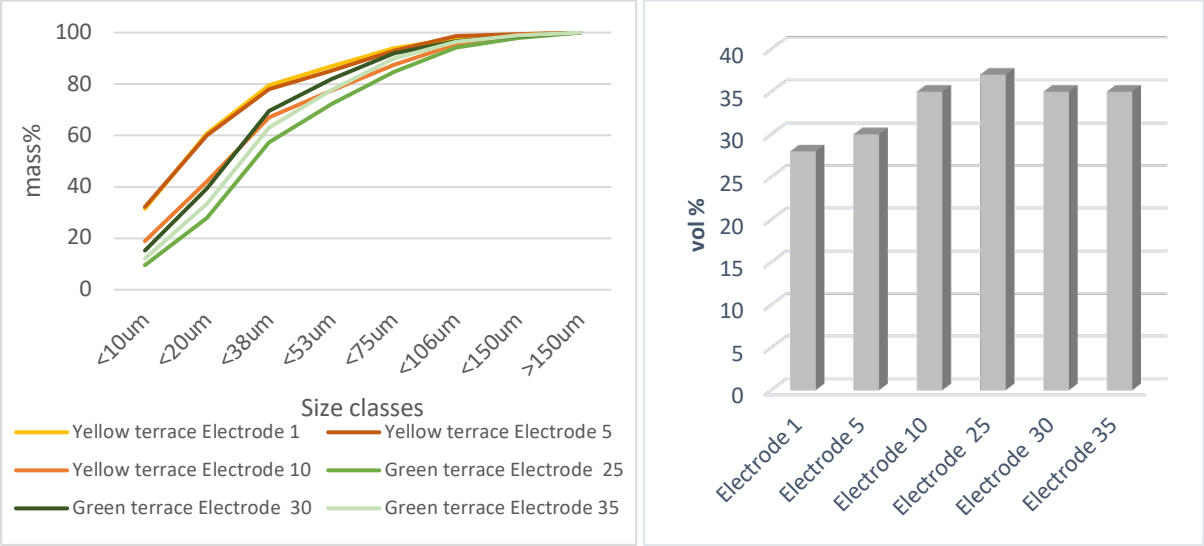

Figure 3. Particle size distribution (left) and water holding capacity (right).

Bulk mineralogy of the selected samples

The selected samples electrodes 1, 5, 10, 25, 30 and 35 are dominated by quartz, followed by clay sulphates, chloritoid and goethite (Figure 4).

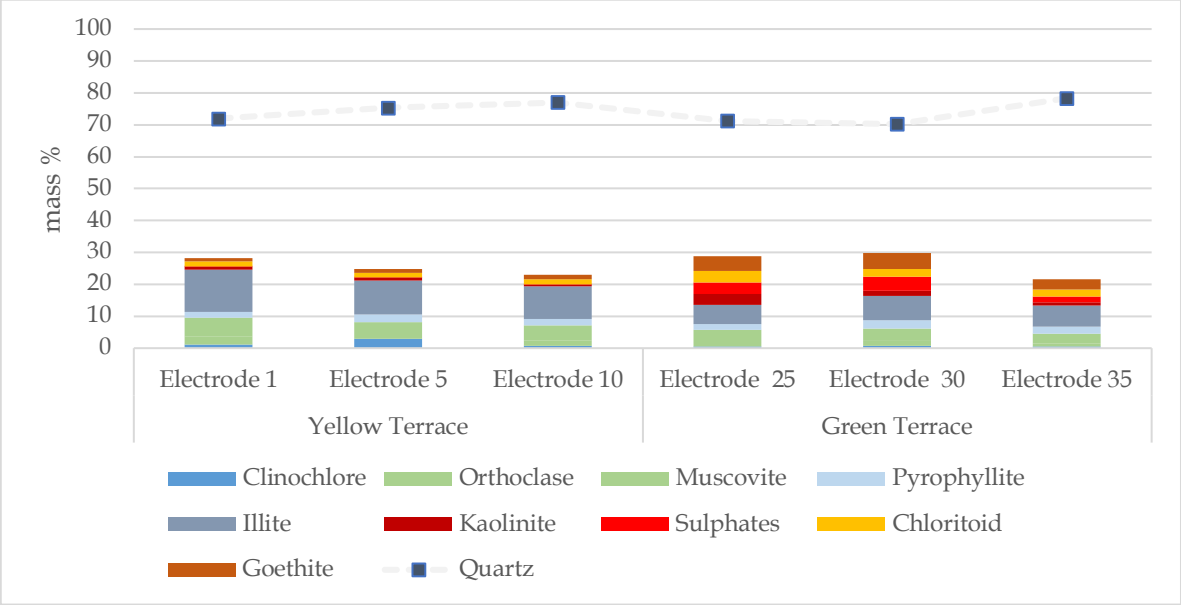

Figure 4. Bulk mineralogy of auger samples.

Clay identified includes illite ($(K,H_3O)(Al,Mg,Fe)_2(Si,Al)_4O_{10}[(OH)_2,(H_2O)]$), kaolinite ($Al\,Si_2O_5OH_4$) and pyrophyllite ($Al_2Si_4O_{10}(OH)_2$). The material analysed was found in the oxidised zone, for this reason, pyrite, the common sulphide in the Witwatersrand Basin, was not identified (Nengovhela, 2006). Birnessite (MnOOH) was identified in trace amounts (less than 1%). The green terrace contains relatively more chloritoid (Fe^{2+}, Mg, Mn^{2+})$Al_2(SiO_4)O(OH)_2$), sulphates, goethite and kaolinite clay. The difference in colour of the two terraces is most likely due to the abundance of chloritoid. Further examination of these phases suggests that the base metals, Cu, Ni, Mn and Zn are mostly hosted by goethite and sulphates (Figure 5). The sulphate particles are quite small – and only a few spots were collected. High clay material is expected to have low resistivities, as clay exhibits high dissolved ion concentration (Hazreek, 2014). However, the metal contents in the clays are not prominent; only gold is found in appreciable amounts in the clays.

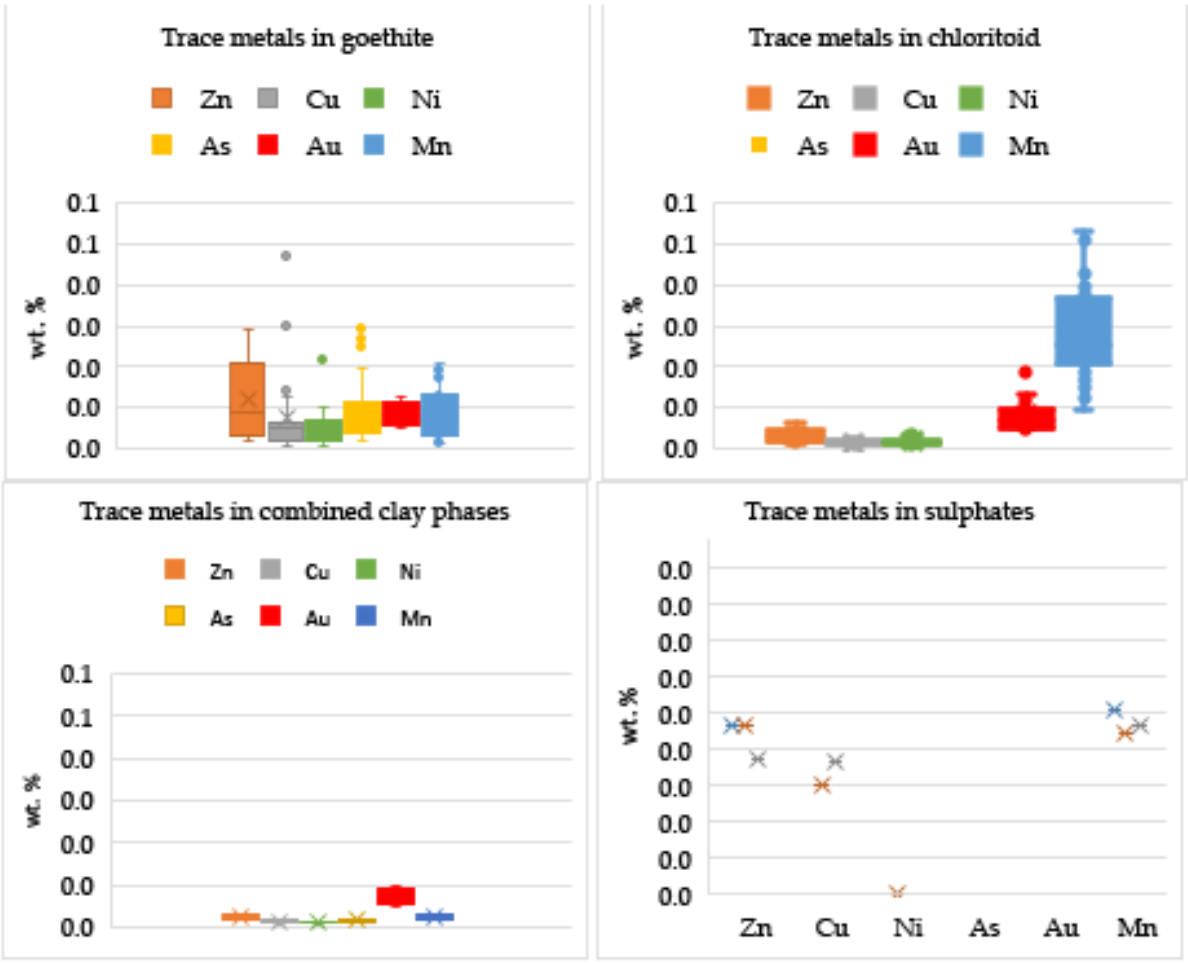

Figure 5. Trace metals are present in major minerals of the auger samples.

Base metal and metalloid distributions

Based on mineralogy, the major elements in the sample are Si and Fe, however tracking of these metals is not of interest and not reported. Gold, base metals and metalloids identified in the Auger samples are listed in Table I.

The concentration of Fe occurs in percentage form, while Au, Zn, Cu, Ni, Pb, As, Mn and V occur in parts per million (ppm). A slightly higher concentration of iron is present in the green terrace. With the exception of Pb, the concentrations of base metals of the yellow terrace are relatively low, with Ni, ranging from 24–34 ppm, Cu from 45-83 ppm, and Zn from 41-48 ppm, while the green terrace has considerably higher values with Ni, ranging from 113 – 158 ppm, Cu from 323- 424 ppm, Zn from 183-404 ppm. Pb follows the same trend as the metalloid As, with higher levels noted in the yellow terrace. Lead in the lower terrace ranges from 115-153 ppm and arsenic ranges from 256 – 347 ppm, while in the green terrace, lead ranges from 68-78 ppm and arsenic is between 145 and 186 ppm.

Table I. Trace metals identified in selected auger samples.

	Analytes	Au	Zn	Cu	Ni	Pb	As	Mn	V	Fe
	Samples	**ppm**								
Yellow terrace	Electrode 1	0.74	48.49	83.16	33.51	153.5	347.24	190.44	47.84	4.40
	Electrode 5	0.70	46.82	63.49	31.88	150.11	313.49	185.17	49.24	4.88
	Electrode 10	0.60	41.25	45.47	24.04	116.6	255.69	172.20	39.26	3.61
Green terrace	Electrode 25	0.54	263.95	323.65	105.13	58.77	145.60	281.02	41.36	5.26
	Electrode 30	0.75	404.50	424.55	158.35	76.42	186.04	333.11	45.50	5.81
	Electrode 35	0.58	183.46	370.05	128.28	70.03	184.53	220.58	42.79	5.50

ERT Calibrations

Pearson correlation analysis, a statistical method used to determine the strength of a relationship between two continuous variables, was used to compare metal content with ERT data (Figure 6). The data points were few, but sufficient to confirm or refute the drivers of electrical conductivity/resistivity.

R-squared was utilised to evaluate the extent to which electrical resistivity in a regression model elucidates the variance in the dependent variable. Its value lies between 0 and 1, with 1 signifying that all the variability in the dependent variable is explained by the independent variables. A higher value of R-squared indicates a superior model fit to the data.

The higher levels of metallic components are consistent with the lower resistivity of the near-surface material of the green terrace. A near one-to-one inverse relationship with log-resistivity is noted for Mn, Ni, Zn, and Cu. Except for Mn, the negative relationship between Zn, Cu, Ni and electrical resistivity may be an attribute of the low theoretical resistivities of Zn (59 n.Ω-m), Cu (16.8 n.Ω-m) and Ni (69.3 n.Ω-m); (O'Connor, 2020). Mn metal follows a similar trend to Zn, Ni and Cu, but has the highest theoretical resistivity value, 1440 n.Ω-m. The resistivity of Mn as metal in this context is immaterial as Mn occurs as oxide. The inter-crystalline and intra-crystalline charge transport processes of Mn oxides are complex, and the electrical properties are variable (Arias, 2019).

Lead and arsenic have high theoretical resistivities, 208 and 333 n.Ω-m (O'Connor, 2019), respectively, but the correlation with log-resistivity in the field was poor (Figure 3). The poor correlation suggests that Pb and As content are not key drivers of electrical resistivity.

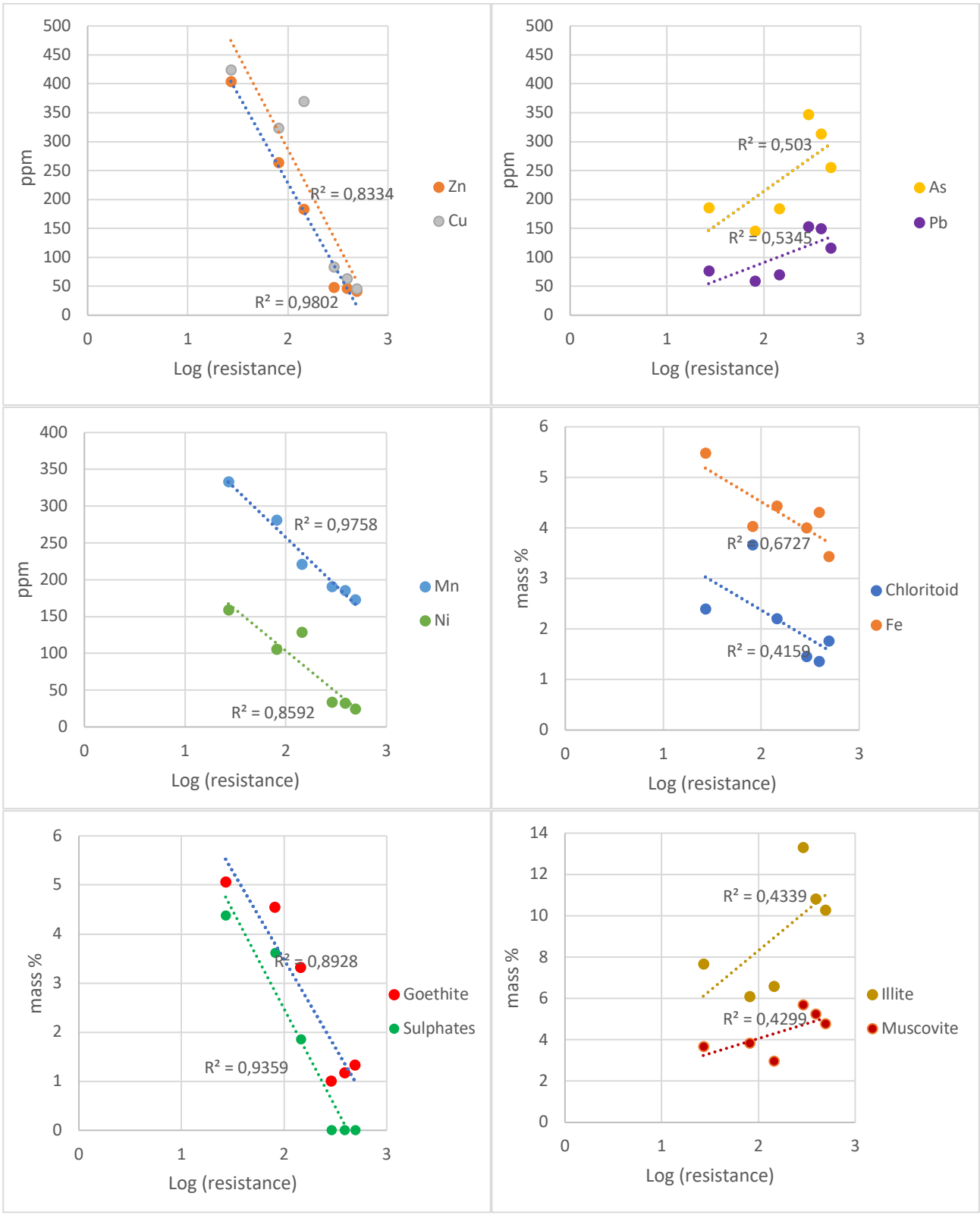

Figure 6. Metal, mineral, and resistance correlation data.

Multivariate analysis

Multi-linear regressions (MLR) were used to understand the impact of each parameter on the electrical resistivity of the auger samples. The regression coefficients (B) were determined by the data (Alexopoulos, 2010). The regression coefficients and residuals were estimated using the Excel data analysis ToolPak. The combinations of variables were evaluated using trial and error of the correlation matrix.

The multi-linear regression model is based on:

$$y= \beta_o+\beta_1 x_1+\beta_2 x_2+\cdots+\beta_k x_ (k)+ \in \quad \text{Equation 1}$$

with Y, the electrical resistivity and x included four variables: goethite, sulphates, copper and nickel. Zinc and goethite had the same response, owing to the zinc deportment.

The following assumptions were made:

- Considering that the particle size distribution of the terraces is similar, the particle size distribution is not likely the reason for the differences in electrical resistivity of the two terraces.
- The material of both terraces was saturated in water with water holding capacity above 20% and slight differences in water content would not affect the current flow.
- Zn, Ni, Cu and Mn concentrations are low but may still affect electrical resistivity significantly. Heavy metal concentrations, as low as 23 ppm, have been predicted using statistical models (Vásconez-Maza *et al.*, (2019). This suggests that the technique is sensitive to very low metal concentrations,
- Goethite has low to moderate resistivity, as it is reactive to water and ions (Yanina & Rosso, 2008).

Table II. Statistical analysis of MLR

	Coefficients	*Standard Error*
Intercept	2.08617	0.09591
Goethite	0.57206	0.08292
Sulphates	-0.61485	0.06255
Copper	0.00039	0.00080
Nickel	-0.00645	0.00205

$$y=2.09+0.57206(\text{goethite})-0.61485(\text{sulphates})+0.0003(\text{copper})-0.00645\ (\text{nickel})+0.09591 \quad \text{Equation 2}$$

The calculated resistivity compares well to the resistivity measured in the field (Figure 7). The data was comparable, however, only six data points were used. The near one-to-one relationship between resistivity, goethite, sulphates, nickel and copper suggests that these variables are drivers of electrical resistivity. Although manganese showed good correlations, it failed to fit the model because it presented in both chloritoid and goethite. Elements are hence not reliable proxies for resistivity. Moreover, the coefficients for goethite and sulphates are high and suggest that minerals, not elements. are the key drivers for electrical resistivity/conductivity.

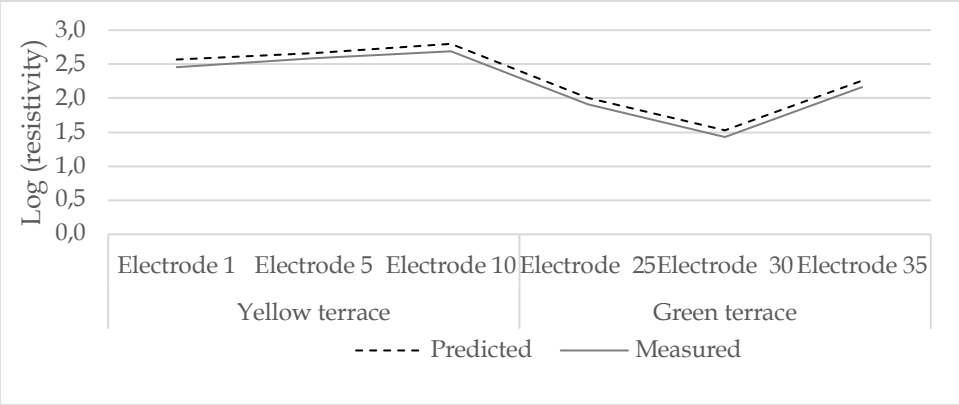

Figure 7. Comparison of experimental and calculated electrical resistivity.

SIGNIFICANCE OF THE METHODOLOGY

The ERT tool is favourable for the site studied, as the extent of oxidation material in the tailings can be inferred from the electrical resistivity data. Sulphates and goethite are products of sulphide oxidation as shown by Equations 2 and 3.

$2FeS_2\,(s) + 7O_2\,(g) + 2H_2O\,(l)\ 2Fe^{2+}\,(aq) + 4SO_4^{2+}\,(aq) + 4H^+\,(aq)$ *Equation 2*

$4Fe^{2+}\,(aq) + O_2\,(g) + 4H^+\,(aq)\ 4\,Fe^{3+}\,(aq) + 2H_2O\,(l)$ *Equation 3*

Oxidation products exhibit low resistivities and are good proxies for acid mine drainage and bioavailable metal. Bioremediation technologies that require exchangeable and acid-soluble species may be identified. The application to bioremediation technologies is promising, as exchangeable and acid-soluble species have been identified. Phytoextraction depends purely on rainwater, a relatively weak lixiviant that targets readily soluble mineral phases (Grover *et al.*, 2016). Sulphates, as well as iron (Fe), and manganese (hydr)oxides identified by ERT, play a significant role in the retention, mobility, and bio-accessibility of both metals and metalloids in soil. Fe/Mn (hydr)oxides can be precipitated and may contribute to metal immobilisation (Mele, 2015). Salts such as sulphates keep clay in a saline state, allowing for good plant structure and permeability to water (Abrol *et al.*, 1988). However high concentrations of sulphate may be detrimental to the plant, rendering less water available to plants and growth of plants may be stunted (Reginato et al., 2021). Plants respond to salinity differently, for example, the growth of tomato plants is not inhibited by high sulphur and sulphate levels (Kowalska, 2005). The plant selection and restoration approaches will hence have to consider the salinity levels of the tailings.

CONCLUSIONS

The application of ERT in TSF characterisation is fairly new and not fully developed for application to restorative agriculture and phytomining. The cost of the technology is low and data processing is relatively quick. This is particularly important for bioremediation projects where funds are limited.

A good comparison is noted between the experimental and calculated electrical resistivity. The higher near-surface bulk conductivity of the green terrace is consistent with the higher levels of metallic components; however, the mineralogy appears to have a greater impact on electrical resistivity. The regression model hence suggests that minerals, not elements, are the key drivers for resistivity. At the time of sampling, moisture had an insignificant effect on resistivity, as the tailings were fully saturated. Particle size also had a minimal effect, as the size distribution was narrow, and particles were very fine.

The tailings characterisation informs the engineering pedogenesis strategy to maximise phytoextraction. In this study, phytoextraction is hence more amenable for the green terrace, as higher metal contents may be readily available for plant uptake.

Finally, this study has provided an understanding of the relationship between mineralogical characteristics and the bioaccessibility of metal(oid)s in the tailings, which is an important parameter for phytoextraction. However, further work is required to validate these findings. ERT surveys across all eight terraces to enhance our understanding of the applicability of the technique are recommended.

ACKNOWLEDGEMENT

The authors would like to thank Mintek for providing financial support to this project.

REFERENCES

Abrol, I. P., J.S.P. Yadav, J.S.P and Massoud, F. I. (1988). Salt-Affected Soils and their Management, FAO Soils Bulletin 39, Food and Agriculture Organization of the United Nations, Rome.

Alexopoulos, E.C. (2010). Introduction to Multivariate Regression Analysis, *Hippokratia* 14(Suppl 1), pp 23-29.

Ahn, Y., Han, M. and Choi, J. (2022). Effect of electrode types and soil moisture on the application of electrical resistivity tomography and time-domain induced polarization for monitoring soil stabilization, *Measurement*, 187.

Arias, N.P., Becerra, M. and Giraldo, O. (2019). Structural and Electrical Studies for Birnessite-Type Materials Synthesized by Solid-State Reactions, *Nanomaterials* 9(8), pp1156-1174.

Fashola, M.O. and Babalola, O.O. (2020). Physicochemical properties, heavy metals, and metal-tolerant bacteria profiles of abandoned gold mine tailings in Krugersdorp, South Africa, *Canadian Journal of Soil Science*, 100(3), pp 1-17.

Gabarrón, M., Martínez-Pagán, P., Martínez-Segura, M.A., Martínez-Martínez, S., Faz, Á. and Acosta, J.A. (2020). Electrical Resistivity Tomography as a Support Tool to Estimate Physicochemical Properties of Mining Tailings Pond, *Minerals*, 10 (559).

Grover, B.P.C., Johnson, R.H. and Tutu, H. (2016). Leachability of metals from gold tailings by rainwater: an experimental and geochemical modelling approach, *Water SA,* 42.

Hazreek, Z.A.M., Aziman, M., Azhar, A.T.S., Chitral, W.S., Fauziah, A. and Rosli, S. (2015). The Behaviour of Laboratory Soil Electrical Resistivity Value under Basic Soil Properties Influences, *IOP Conference Series: Earth and Environmental Science*, 23.

Jodry, C., Palma Lopes, S., Fargier, Y., Martin Sanchez, M. and Côte, P. (2019). 2D-ERT monitoring of soil moisture seasonal behaviour in a river levee: A case study, *Journal of Geophysics*, 167, pp. 140-151.

Kapaj, S., Petersen, H. and Liber, K. (2006). Human Health Effects from Chronic Arsenic Poisoning–A Review, *Journal of Environmental Science and Health Part A* 41(10):2399-428.

Kawolska, I. (2005). Effects of sulphate level in the nutrient solution on plant growth and sulphur content in tomato plants, *Folia Horticulturae Ann*. 17/1, pp 91-100.

Lyu, J., Hu, Y., Ren, S., Yao, Y., Ding, D., Guan, Q. and Tao, L. (2021). Extracting the tailings ponds from high spatial resolution remote sensing images by integrating a deep learning-based model, *Remote Sense*, 13, 743.

O'Connor, J. (2020). Electrical Resistivity and Electrical Conductivity, available from https://www.periodic-table.org, accessed 8 June 2023.

Maurya, P.K, V.K. Rønde, V.K., Fiandaca, G., Balbarini, N., Auken, E., Bjerg, P.L. and Christiansen, A.V. (2017). Detailed landfill leachate plume mapping using 2D and 3D electrical resistivity tomography - with correlation to ionic strength measured in screens, *Journal of Applied Geophysics*, 138, pp1-8.

Mele, E., Donner, E., AJuhasz, A.L., Brunetti, G., Smith, E., Betts, A. R., Castaldi, P. Deiana, S., Scheckel, K. G. and Lombi, E. (2015). In Situ Fixation of Metal(loid)s in Contaminated Soils: A Comparison of Conventional, Opportunistic, and Engineered Soil Amendments, *Environ. Sci. Techno*, 49, pp 13501−13509.

Minerals Council South Africa (2019). Environment and Legacy Issues, available from *https://www.miningforschools.co.za/lets-explore/gold/environment-and-legacy-issues*, accessed 1 August 2021.

Nengovhela, C., Yibas, B. and Ogola, J.S. (2006). Characterisation of gold tailings dams of the Witwatersrand Basin with reference to their acid mine drainage potential, Johannesburg, South Africa, *Water SA*, (32) 4.

Netshiongolwe, K. (2018). Geochemical characterisation of gold tailings footprints on the Central Rand Goldfield, *Environmental Science*, available from https://www.semanticscholar.org/paper/Geochemical-characterisation-of-gold-tailings-on-Netshiongolwe/467841d598e615688b2d92b56a56b0930ac77b2f/figure/1, accessed from 1 August 2021.

Martínez-Pagán, P., Gómez-Ortiz, D., Martín-Crespo, T., Martín-Velázquez, S. and Martínez-Segura, M. (2021). Electrical Resistivity Imaging Applied to Tailings Ponds: An Overview, *Mine Water and the Environment*, 40, pp 285–297.

Reginato, M., Luna, V. and Papenbrock, J. (2021). Current knowledge about Na_2SO_4 effects on plants: What is different in comparison to NaCl? *J Plant Res*, **134**, pp 1159–1179. https://doi.org/10.1007/s10265-021-01335-y.

Yanina, S. V. and Rosso, K.M. (2008). Linked Reactivity at Mineral-Water Interfaces through Bulk Crystal Conduction, *Science*, New Series, 320 (5873), pp. 218-222, American Association for the Advancement of Science.

Marian Merle Manuel

Executive Manager: mineralogy
Mintek

Marian has 17 years of experience in mineralogy, with qualifications in both geology (University of Witwatersrand) and metallurgy (University of Pretoria). She started her career at Mintek in 2005, as a scientist in training but has worked for Anglo American and Exxaro as a process mineralogist. Her professional research interests focus on predictive modelling and waste valorization. She is pursuing her PhD at the University of Cape Town in partnership with the Centre for Bioprocessing Engineering Research.